Computation of the effective area and associated uncertainties of non-rotating piston gauges FPG and FRS

OPEN ACCESS
IOP Publishing | Bureau International des Poids et Mesures Metrologia

Metrologia **56** (2019) 015004 (10pp) https://doi.org/10.1088/1681-7575/aaee18

Computation of the effective area and associated uncertainties of non-rotating piston gauges FPG and FRS

Steryios Naris[1,5], Nikos Vasileiadis[1], Dimitris Valougeorgis[1], Ahmed S Hashad[2,4] and Wladimir Sabuga[3]

[1] Department of Mechanical Engineering, University of Thessaly, Pedion Areos, Volos 38334, Greece
[2] National Institute for Standards (NIS), 136 Giza, 12211, Egypt
[3] Physikalisch-Technische Bundesanstalt (PTB), Bundesallee 100, Braunschweig 38116, Germany

E-mail: snaris@mie.uth.gr

Received 30 July 2018, revised 29 October 2018
Accepted for publication 5 November 2018
Published 30 November 2018

Abstract

The effective areas of three force-balanced piston gauges (FPGs) and two Furness Rosenberg standards (FRS) in the operating pressure range of each device varying for 1 Pa–15 kPa have been accurately computed both in the gauge and absolute modes. Geometrical data for the non-rotating piston-cylinder assemblies (PCAs) have been provided by the National Metrology Institutes (NMIs) of PTB, RISE, INRiM and CMI. Since the flow is in a wide range of the Knudsen number, simulations have been based on the Batnagar–Gross–Krook (BGK) kinetic model equation, while the typical Dadson and CFD approaches have been complimentary applied only in the viscous regime. Furthermore, an uncertainty analysis has been performed. The effective area is strongly affected by the PCA geometry and the flow conditions, while its dependency on pressure may be different even for devices of the same type. The main source of uncertainty is the dimensional measurements of the piston and the cylinder, followed by the accommodation coefficient characterizing the gas-surface interaction, while the effect of other flow and modeling parameters is negligible. The total relative standard uncertainty of the effective area has been always found to be less than $1 \cdot 10^{-5}$ indicating that pressure measurements of high accuracy can be ensured. Since the effective area is estimated based solely on computations the FPG and the FRS assemblies may be characterized as primary pressure standards.

Keywords: primary pressure standard, effective area, rarefied gas dynamics, FPG and FRS characterization

(Some figures may appear in colour only in the online journal)

1. Introduction

In many industrial sectors, such as cleanroom technologies, petrochemicals, pharmaceuticals, storage of nuclear and toxic wastes and power plants, the pressure range between 1 Pa and 15 kPa is present in various stages of the production lines. The accuracy and reliability of the pressure measuring devices are critical and have to be ensured. Pressure standards of high accuracy, capable of providing traceability at sufficient low uncertainty level following the demands of industry are required.

In the specific pressure range, however, there is a lack of fundamental standards that can provide the required accuracy. Some of the promising devices that could be used as primary

[4] Guest researcher at PTB.
[5] Author to whom any correspondence should be addressed.

standards in the pressure range 1 Pa–15 kPa are piston gauges (PGs) equipped with the non-rotating piston-cylinder assemblies (PCAs) [1–5]. In the present work, two of these devices are examined. The first one is the force-balanced piston gauge FPG8601, manufactured by Fluke, which is used by many National Metrology Institutes (NMIs) and pressure calibration laboratories as a reference instrument for both absolute and gauge modes [3, 6]. The second one is the Furness Rosenberg standard (FRS), manufactured by Furness Controls [7], which is also used by various NMIs and calibration laboratories, and has been also proved as a reference and transfer standard for low absolute and gauge pressures [8]. Two different types of FRS instruments, namely the FRS4 and FRS5, are in use by laboratories.

In the previous years, comparisons between NMIs have been performed targeting at the statement of equivalence between pressure standards [3, 4, 8], but only few attempts to characterize the FPG8601 or FRS as primary standards have been reported [9–12]. In order to metrologically characterize each device, all parameters that can affect the measurement have to be examined and quantified. The most important parameter is the effective area (A_{eff}) of the PCA. Per definition, the effective area of a PCA is the net force acting on the piston in course of the measured pressure divided by the value of this pressure. This net force includes, among others, the forces acting on the piston due to the gas flow in the gap between the piston and the cylinder. These forces have to be calculated based on the real geometry of the gap and using suitable simulation tools to find out the pressure distribution in the piston-cylinder gap with high accuracy and reliability. Then, the effect of the flow can be combined with the geometrical surface of the piston to recover A_{eff}. When the PCA is planned to be used as a primary standard, the effective area has to be estimated based on geometrical data in a very accurate and precise manner.

It is noted that the dimensions of the gap between the piston and the cylinder, in both the FPG and FRS devices, are of the order of micrometres (μm). In addition, the operational pressure is small, especially when the devices are working in absolute mode. Under these conditions, there are regions in the flow domain where the mean free path between two molecular collisions is comparable to the characteristic length of the flow and the typical approaches of fluid dynamics such as the Navier–Stokes equations or simplified theories, such as the Dadson theory [13], cannot describe the flow with accuracy. Alternative simulation tools based on kinetic theory and modeling as described by the Boltzmann equation (BE) [14, 15] are needed.

Using kinetic model equations produced by simplifications of the BE is a reliable option producing very accurate results. This approach has been implemented for many decades in the simulation of rarefied gas flows either at low pressure conditions [16, 17] or in microdevices [18, 19] with considerable success. More specifically, the Bhatnagar–Gross–Krook (BGK) kinetic equation, where the collision term of the BE is replaced with a simplified model expression, has been applied in various pressure driven flow configurations and produced excellent results, especially when isothermal flows are examined. This approach is valid in the whole range of the Knudsen number which allows the flow to be simulated in a unified manner without the need of combining meso- and macroscale (viscous) approaches. Recently, the same methodology has been applied for simulation of gas flow in pressure measuring standards [12, 20, 21].

In the present work, a detailed computational investigation of the gas flow in PCAs is performed via the BGK kinetic model approach and the effective area of the PCAs is computed in the whole range of the operational pressure for both the gauge and absolute modes. The methodology is applied to three different FPG8601, as well as to one FRS4 and to one FRS5. The geometrical data for the three FPGs have been provided by NMIs PTB (Germany), RISE (Sweden) and INRiM (Italy), while for the FRS4 and FRS5 by CMI (Czech Republic) and PTB, respectively. Furthermore, the uncertainties due to measurements as well as to the various flow conditions and parameters are considered and their effect on the computed effective area for each device is provided.

2. Description of devices

The main characteristics of the FPG8601, the FRS4 and the FRS5 are well-known and therefore, only a brief description is provided here pointing the issues which are of importance in the present work. In figure 1, a schematic representation of the three investigated PCAs is shown. In all three devices, two parts of the gap can be clearly identified, namely the top and bottom parts. The dimensional data of all PCAs include the piston radius r_i, the cylinder radius R_i, the gap width h_i and the piston-cylinder engagement length L_i, where $i = \text{T}$ and $i = \text{B}$ correspond to the top and bottom parts, respectively. In addition, P_{meas} is the measured pressure, P_{ref} is the reference pressure, while in the FPG8601 configuration, P_{lub} is the pressure of the lubrication gas entering the piston-cylinder gap.

The main part of the FPG8601, manufactured by Fluke, is the PCA, which is located between two pressure chambers, namely the measuring and the reference chambers [1, 6, 22]. The former contains the gas under investigation, while the latter one remains at a reference pressure against which the measured gas pressure is defined. The operating pressure range is between 1 Pa–15 kPa and depending on the reference pressure (100 kPa and 1 Pa in the gauge and absolute modes respectively), measurements can be performed in either mode. The piston and the cylinder are separated by a biconical gap with a nominal width of 6 μm at the PCA center and 1 μm at the two PCA extremities. This gap is used to avoid frictional forces and to keep the piston aligned via a lubricating gas flow. The lubricating gas enters the piston-cylinder gap through two supply holes located at the cylinder center at a pressure 40 kPa higher than the reference pressure and flows towards the two pressure chambers. Finally, a high precision load cell measures the force acting on the piston, and the pressure of the investigated gas is extracted by using the piston-cylinder effective area.

The PCA of the FRS4 [23], manufactured by Furness Controls, is also located between the measuring and reference

pressure chambers. The FRS4 operates only in the gauge mode and has a measuring pressure range between 1 Pa–3.2 kPa. The piston and cylinder have constant diameters and a nominal gap width of 50 μm [7]. Friction between the piston and cylinder is avoided by using a parallelogram suspension system with flexible hinges, which ensures no relative horizontal displacement of the piston but allows free axial movement. Gas is supplied from an annular groove located at the top of the PCA, while almost all the gas is extracted before reaching the reference pressure (100 kPa) chamber through the intermediate port annular groove located at the PCA bottom. Finally, the PCA is mounted on an electronic balance mechanism, which can give a precise value of the force acting on the piston.

The FRS5 is a more recent version of the FRS4. The most important change is the ability to operate in both gauge and absolute modes with the reference pressure chamber kept at 100 kPa and 0.01 Pa, respectively, while the operating pressure range is extended to 1 Pa–11 kPa. Other modifications include the capability of checking the zero setting without evacuation and an additional turbo molecular pump for the working volume, while the gap between the piston and the cylinder is reduced to a nominal value of 25 μm [5]. Also, the nominal piston area is reduced from about 100 cm^2 to about 45 cm^2. More details on the design and operation of the devices can be found in the literature [5, 7, 23].

3. Method of calculation of effective area and the associated uncertainties

The accuracy of the pressure measurement of the three investigated piston gauges mainly depends on the precision of the force measurement and the accuracy of the computed effective area. The latter one is the main objective of this work. The effective area of a PCA is defined as the ratio of the force F_{read} acting on the piston over the pressure difference between the two piston ends

$$A_{\mathrm{eff}} = \frac{F_{\mathrm{read}}}{P_{\mathrm{meas}} - P_{\mathrm{ref}}}. \tag{1}$$

The operational data of the FPG8601 include the measuring, lubrication and reference pressure values, while for the FRS4/5 the operational data are the measuring, intermediate and reference pressure values. The effective area of each part is computed separately by taking into account the forces that act on each part respectively. These forces include: (a) the force due to the pressure difference, (b) the drag force due to the lubricating gas flow and (c) the vertical component of the pressure force that acts normally to the piston lateral surface. Since the ratio of the gap width over the radius of the piston h/r is sufficiently small then the effective area can be expressed as [13]

$$A_i = \pi r_{0,i}^2 \left(1 + \frac{h_{0,i}}{r_{0,i}} - \frac{1}{r_{0,i}\left(P_{\mathrm{in},i} - P_{\mathrm{out},i}\right)} \int_0^{L_i} \left(R_i - R_{0,i} + r_i - r_{0,i}\right) \frac{\mathrm{d}P_i}{\mathrm{d}z_i} \mathrm{d}z_i\right). \tag{2}$$

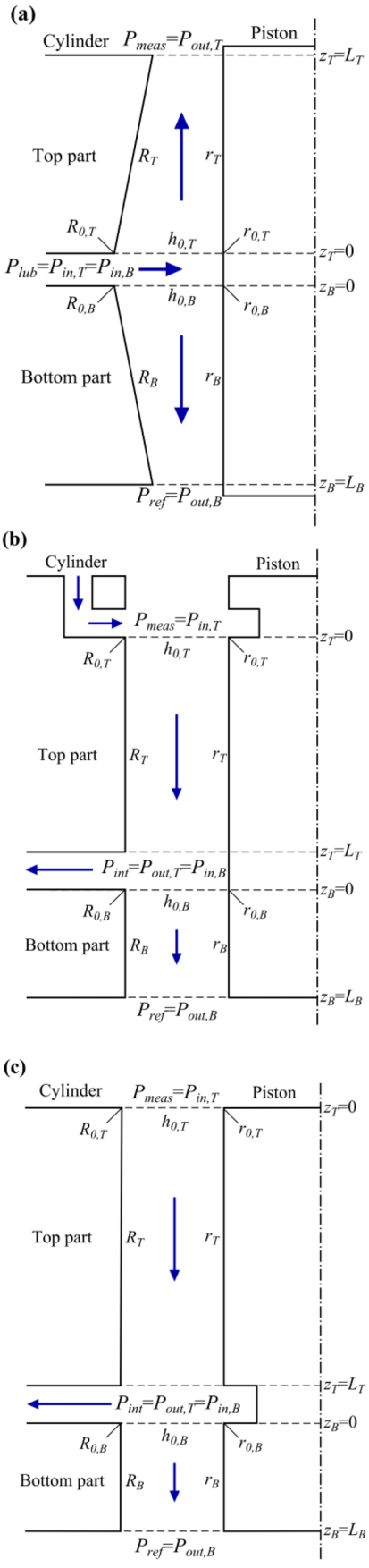

Figure 1. Schematic representation of (a) FPG8601, (b) FRS4 and (c) FRS5 cross sections.

Table 1. Geometrical data of the three FPG8601s provided by PTB, RISE and INRiM.

FPG assembly	PTB		RISE		INRiM	
FPG Part	Top	Bottom	Top	Bottom	Top	Bottom
Number of angular positions	8	8	8	8	4[a]	4[a]
Number of axial points	343	339	317	346	69	69
Engagement length (mm)	34.2	33.8	31.6	34.5	34.0	34.0
Average gap inlet width (μm)	4.646	4.414	3.889	3.784	4.238	4.131
Average gap width (μm)	2.511	2.551	2.617	2.490	2.474	2.486
Average gap outlet width (μm)	2.013	2.155	1.015	1.553	1.087	0.922
Average piston radius (mm)	17.6664	17.6664	17.6658	17.6658	17.6658	17.6658
Average cylinder radius (mm)	17.6689	17.6689	17.6684	17.6683	17.6683	17.6683
Average piston area (cm^2)	9.804 96	9.804 94	9.804 31	9.804 33	9.804 33	9.804 32
Diameter uncertainty (nm)	25	25	200	200	26	26

[a] INRiM data are based on diameter measurements only and, herewith, the radial values for angles 0°, 45°, 90° and 135° are the same as for angles 180°, 225°, 270° and 315°.

In the FPG8601, the total effective area can be computed by taking into account the forces F_T and F_B that act on the top and bottom piston parts, respectively, during pressure measurement, as well as the taring force F_0 acting on the piston due to the load cell zeroing process. The total force that acts on the piston is $F = F_B – F_T – F_0$ and after some mathematical manipulation of equation (1), the total effective area of the FPG8601 can be calculated as

$$A_{\text{eff}} = \frac{P_{\text{meas}} A_T - P_{\text{ref}} A_{T,0}}{P_{\text{meas}} - P_{\text{ref}}} - \frac{P_{\text{lub}} \left(A_T - A_{T,0}\right)}{P_{\text{meas}} - P_{\text{ref}}} \tag{3}$$

where $A_{T,0}$ is the effective area of the top part during the load cell zeroing process. In the FRS4/5, the total effective area is computed in the same manner. Here, the total force F is the addition of the force that acts on the top part F_T and the force that acts on the bottom part F_B. It is readily seen that the total effective area can be written as

$$A_{\text{eff}} = A_T + \frac{P_{\text{int}} - P_{\text{ref}}}{P_{\text{meas}} - P_{\text{ref}}} \left(A_B - A_T\right). \tag{4}$$

It is observed that, when the dimensional data of the PCA are known, only the pressure distribution along the gap must be defined in order to calculate the effective area. In the hydrodynamic regime, the analytical solution of the Poiseuille flow for a compressible ideal gas provides the pressure distribution in a closed form [13]

$$P_i\left(z_i\right) = \left[P_{\text{in},i}^2 - \left(P_{\text{in},i}^2 - P_{\text{out},i}^2\right) \frac{\int_0^{z_i} h_i^{-3} \mathrm{d}z_i}{\int_0^{L_i} h_i^{-3} \mathrm{d}z_i}\right]^{1/2}. \tag{5}$$

However, due to the low operating pressure and the small gap dimensions, the continuum hypothesis collapses and the hydrodynamic solution is not valid. In this case, a kinetic approach is required to calculate the pressure distribution along the gap. It is important to note, that the kinetic results are also valid for the hydrodynamic regime and thus, the kinetic theory can be applied as a uniform method.

In the kinetic formulation, the pressure drop along the gap is computed by solving the ordinary differential equation [24]

$$\frac{\mathrm{d}P_i}{\mathrm{d}z_i} = \frac{\dot{M}_i u_0}{2\pi G h_i \left(R_i^2 - r_i^2\right)} \tag{6}$$

subject to the known pressure at the inlet and the outlet of the gap defined by P_{in} and P_{out}, respectively. Here, u_0 is the most probable molecular speed and $G(\delta, r/R)$ is the dimensionless flow rate.

An iterative scheme is applied, where an initial guess of mass flow rate is used to find the pressure distribution along the gap and the pressure at the outlet. Then, depending on the deviation between the calculated and real value of the pressure at the outlet, a new guess of the mass flow rate is used and the computational process is repeated. The iterative scheme is ended when the outlet pressure is recovered with a relative error smaller than 10^{-7}.

As it is clearly seen from equation (6), the value of the dimensionless flow rate G is needed on each step of the process. Since G depends on both the rarefaction parameter δ, which is inversely proportional to the Knudsen number, and the ratio r/R between the piston and the cylinder radii, a robust kinetic database is needed. For the present study, a dense database has been created by solving the linearized BGK kinetic model equation for different values of $\delta \in [10^{-10}, 10^4]$ and $r/R \in [0.99, 0.999\,99]$ with the accommodation coefficient, characterizing the gas-surface interaction, taking the values of $\alpha = [1, 0.9, 0.8]$. It is noted that $\alpha = 1$ corresponds to purely diffuse reflection, while the values of $\alpha < 1$ correspond to diffuse-specular reflection.

Dimensional measurements have been performed by the PTB, INRiM, RISE and CMI. Depending on the available equipment and method of measurement, different level of uncertainty is achieved and consequently, the effective area calculation is subjected to a proportional level of uncertainty. Since dimensional data are needed for both the piston and the cylinder components, the standard uncertainty of the effective area of the PCA due to the measurement uncertainty denoted by u_d is estimated as [20]

$$\frac{u_d\left(A_{\text{eff}}\right)}{A_{\text{eff}}} = \frac{\sqrt{u_p^2 + u_c^2}}{2R_m} \tag{7}$$

where u_p and u_c are the values of the diameter uncertainties of the piston and cylinder, respectively, while R_m is the mean piston and cylinder radius. This equation assumes the dimensional uncertainties of the piston and cylinder to be uncorrelated, which is justified by an analysis of the dimensional data's uncertainty presented in [25].

Table 2. Geometrical data of FRS4 and FRS5 provided by CMI and PTB, respectively.

FRS assembly	FRS4 (CMI)	FRS5 (PTB)	
FRS part	Top	Top	Bottom
Number of angular positions	8	8	8
Number of axial points	2001	882	1
Engagement length (mm)	40.00	44.05	7.95
Average gap inlet width (μm)	34.038	58.842	30.200
Average gap width (μm)	33.412	31.683	30.200
Average gap outlet width (μm)	31.825	58.287	30.200
Average piston radius (mm)	56.418 41	37.985 09	37.985 56
Average cylinder radius (mm)	56.451 82	38.016 78	38.015 76
Average piston area (cm^2)	100.0015	45.329 02	45.330 12
Diameter uncertainty (nm)	500	25	25

In addition to the dimensional measurements, there are tentative variations in other parameters that can increase the overall uncertainty of the effective area and are mostly connected to the deduced flow field and pressure distribution along the gap. These parameters include the accommodation coefficient α, the gas temperature T, the modeling error due to the implementation of the BGK model instead of the original BE and the approximation of introducing in the computations dry N_2 instead of N_2 with some humidity. In order to have the maximum possible change in the computed effective area due to these parameters, when the exact values are not known, the worst-case scenario is adopted. For each parameter, the uncertainty introduced is calculated based on the relative deviation of the effective area computed based on the reference case scenario. The reference data are: $\alpha = 1$, $T = 20$ °C, pure dry nitrogen and BGK model. For each case, only the parameter under investigation is changed, while the rest of the parameters remain as in the reference case. The uncertainty of the effective area of the device due to uncertainty of parameter j is denoted by u_j and is estimated as

$$\frac{u_j\left(A_{\text{eff}}\right)}{A_{\text{eff}}} = \frac{\Delta_j\left(A_{\text{eff}}\right)}{A_{\text{eff}}}. \tag{8}$$

The subscripts $j = \alpha, t, m, h$ correspond to the accommodation coefficient, temperature, model equation and humidity uncertainties respectively, while $\Delta_j(A_{\text{eff}})$ is the difference between the effective area of the reference case and the case under investigation. Finally, the overall uncertainty is calculated as the Euclidean norm of all investigated uncertainties:

$$\frac{u\left(A_{\text{eff}}\right)}{A_{\text{eff}}} = \left[\sum_j \left(\frac{u_j\left(A_{\text{eff}}\right)}{A_{\text{eff}}}\right)^2\right]^{0.5}, \qquad j = d, \alpha, t, m, h. \tag{9}$$

In sections 4.2 and 4.3, the computed effective areas and the associated uncertainties are provided for each PCA. All uncertainties in this publication are standard uncertainties.

4. Results and discussion

Numerical simulations have been performed for all 5 PCAs based on the dimensional datasets provided by the NMIs (PTB, RISE, INRiM and CMI). The kinetic algorithm used has been validated through comparison with other in-house mesoscale tools including the DSMC method, while comparison with the hydrodynamic approach has been also successfully performed for high operation pressure test cases. In addition, PTB has developed in parallel and independently numerical codes using both the Dadson theory and the BGK kinetic equation obtaining excellent agreement between corresponding results for both PTB devices.

4.1. Data of the FPGs and FRS4/5

In tables 1 and 2, the basic parameters of the datasets for the FPG8601s and the FRS4/5 are tabulated, respectively. The data include information about the number and position of the dimensional data provided for the analysis (number of angular positions of measurement and number of axial points), the total engagement length, the average gap measurements (inlet, outlet, mean), the average piston and cylinder radii and the average piston area. The uncertainty of the diameter measurements is also provided. As it is seen, PTB and INRiM devices have similar diameter uncertainties, while RISE and CMI have much higher diameter uncertainties resulting in a higher dimensional uncertainty.

The FPG8601 assemblies of PTB and RISE have similar resolution in the axial direction and both have eight points in the azimuthal direction. On the other hand, the INRiM assembly has fewer points on the axial direction and 4 points in the azimuthal direction. This difference of the resolution of measurements can be attributed to different equipment used or to different processing of the original dimensional measurement results.

For the FRS4, data have been provided only for the top part and not for the bottom part of the PCA due to technical reasons. However, based on the operational principle of the device, it can be assumed that there is no flow in the lower part since the bulk of the gas is extracted from the lower groove and consequently, there are no forces acting on the piston due to gas flow in the lower part.

In all simulations, dry N_2 at 20 °C has been used as the working fluid. No end effects have been considered for the gas flow since the ratio of the length over the average gap width is very large for all devices (about 4000 for FPG8601 and 1000 for FRS). It has been proved that, under such conditions, end effects are negligible [26].

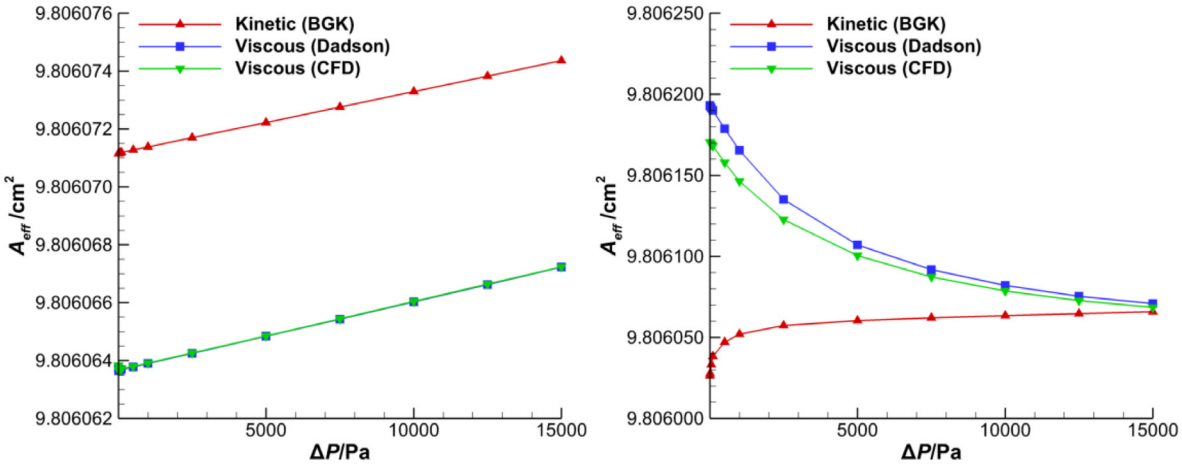

Figure 2. Effective area of FPG8601 of PTB for gauge (left) and absolute (right) mode.

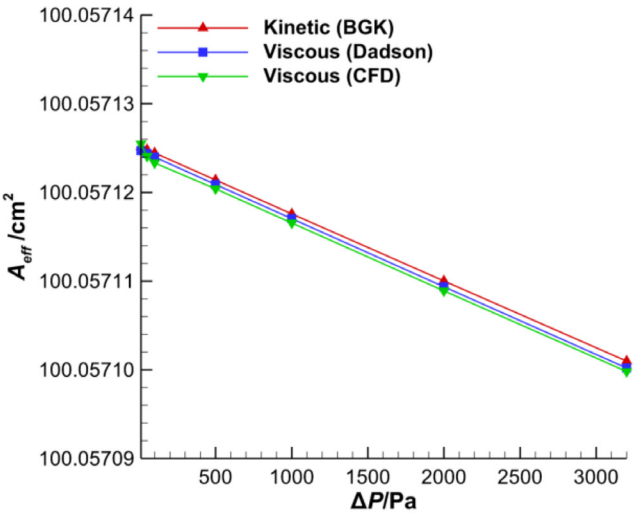

Figure 3. Effective area of FRS4 for gauge mode.

4.2. Computation of effective area

Simulations have been performed for all 5 PCAs at each angular position according to the data in tables 1 and 2, and each time the effective area has been calculated, considering a device as axisymmetric with constant radii in the azimuthal direction for both piston and cylinder. Then, the overall A_{eff} is recovered as the average of all angular values. In all cases, the effective area results are provided with respect to the pressure difference (ΔP) which is defined as the difference between the measured absolute pressure and the reference absolute pressure, the latter being 100 kPa for the gauge mode and 0 Pa for the absolute mode.

To test the range of applicability of all available numerical tools, simulations using the BGK kinetic equation, Dadson theory and the CFD algorithm have been carried out, and a comparison is performed to test the range of validity of the viscous approaches (Dadson and CFD). Results are presented in figures 2–4 for the FPG8601 of PTB, the FRS4 and the FRS5, respectively. A comparison between the effective areas computed by the kinetic and viscous approaches is provided first in the gauge mode and then in the absolute mode.

In the gauge mode of the FPG device (figure 2), there are significant discrepancies between the kinetic approach and the two viscous approaches. This is contributed to the small width of the gap in the FPG, which is about 2–4 μm, resulting, especially at the end of the piston-cylinder engagement length where both pressure and gap width are reduced, to rarefied conditions. As it is well known in such conditions the Knudsen number is relatively large and the viscous approaches are not valid. On the contrary, very good agreement between the effective areas of the kinetic and viscous approaches is observed in the gauge mode of the FRS4 (figure 3) and FRS5 (figure 4) devices. In both FRS, the gap width is of the order of tens of mircometres and the flow is mostly in the hydrodynamic and (partially) in the slip regimes. Consequently, in the gauge mode, the kinetic approach is valid for all PCAs, while the Dadson and CFD approaches are applicable only for the FRS devices.

In the absolute mode of the FPG (figure 2) and FRS5 (figure 4), the discrepancies between the kinetic approach and the two viscous approaches are always significant, and this is due to the low pressures with the gas flow being in the transition and free molecular regimes. Under such rarefied conditions, only the kinetic methodology can provide reliable and accurate results. Even when the pressure is increased and the deviations between the kinetic and viscous approaches are reduced, the viscous approaches cannot be implemented because the exact pressure at which gas rarefaction effects start to appear is not known *a priori* and it varies at each device. Consequently, in the absolute mode, the viscous approaches are not applicable. Therefore, the results presented here are based on the kinetic approach since it is the only one that should be applied for both modes and all devices.

Closing this discussion, it is noted that comparing the effective areas of the FPGs of RISE and INRiM, based on the kinetic and viscous approaches, yields a similar behavior with the one observed in figure 2 for the FPG of PTB and therefore, these plots are omitted.

In table 3 the effective area A_{eff} for the three FPG devices is tabulated, in the absolute and gauge mode operation. The respective results for the two FRS devices are presented in

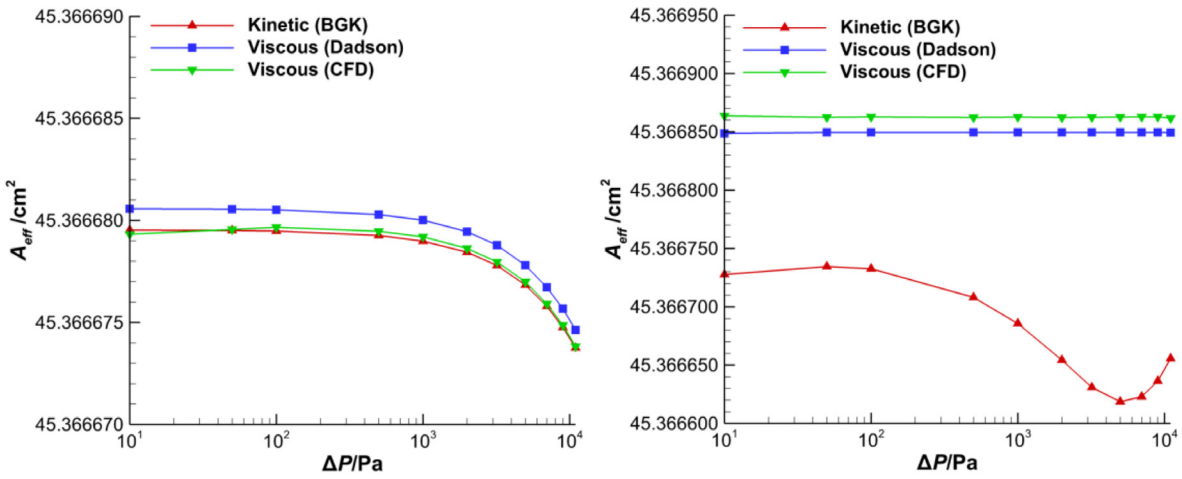

Figure 4. Effective area of FRS5 for gauge (left) and absolute (right) mode.

Table 3. Effective area (cm^2) of the three FPG assemblies in the gauge and absolute modes.

	Gauge mode			Absolute mode		
ΔP/Pa	PTB	RISE	INRiM	PTB	RISE	INRiM
2	9.806 0712	9.805 0698	9.805 1821	9.806 0260	9.805 2474	9.805 2480
10	9.806 0712	9.805 0699	9.805 1822	9.806 0277	9.805 2462	9.805 2479
100	9.806 0712	9.805 0699	9.805 1822	9.806 0383	9.805 2405	9.805 2447
1000	9.806 0714	9.805 0703	9.805 1827	9.806 0519	9.805 1929	9.805 2307
2500	9.806 0717	9.805 0710	9.805 1837	9.806 0573	9.805 1607	9.805 2154
5000	9.806 0722	9.805 0722	9.805 1852	9.806 0604	9.805 1389	9.805 2040
7500	9.806 0728	9.805 0734	9.805 1868	9.806 0621	9.805 1286	9.805 1980
10 000	9.806 0733	9.805 0746	9.805 1883	9.806 0635	9.805 1225	9.805 1951
12 500	9.806 0738	9.805 0758	9.805 1898	9.806 0647	9.805 1188	9.805 1940
15 000	9.806 0744	9.805 0770	9.805 1914	9.806 0658	9.805 1166	9.805 1939

Table 4. Effective area (cm^2) of the FRS4/FRS5 assemblies in the gauge and absolute modes.

	Gauge mode		Absolute mode
ΔP/Pa	FRS4 (CMI)	FRS5 (PTB)	FRS5 (PTB)
1	100.057 12	45.366 680	45.366 700
10	100.057 12	45.366 680	45.366 728
100	100.057 12	45.366 679	45.366 733
1000	100.057 12	45.366 679	45.366 686
2000	100.057 11	45.366 678	45.366 654
3200	100.057 10	45.366 678	45.366 631
5000	—	45.366 677	45.366 619
7000	—	45.366 676	45.366 623
9000	—	45.366 675	45.366 636
11 000	—	45.366 674	45.366 656

table 4. As pointed in section 2, the pressure range varies in each device depending on its maximum operating pressure. More specifically, the maximum operating pressure of the FPG8601, the FRS4 and the FRS5 is 15 kPa, 3.2 kPa and 11 kPa, respectively.

In the gauge mode for all FPG8601 devices, the effective area increases as the operating pressure is increased. However, in the absolute mode, the effective area of the FPG of PTB is increased with the operational pressure, while it is decreased for the other two FPGs of RISE and INRiM. The effective area of both FRS4/5 is slightly decreased as the operating pressure is increased in the gauge mode. For the FRS5 in the absolute operational mode the effective area is not changed monotonically with pressure. Initially, it increases with operational pressure changing from 10 Pa to 100 Pa, then it decreases with operational pressure rising to 5 kPa and then, it increases again. As it is seen, there is no clear trend of the effective area with respect to the operating pressure, and this is true for all devices (including the three FPGs).

Based on the tabulated results in tables 3 and 4, it is concluded that the effective area is strongly affected by the geometry of the device and the flow conditions. Even for devices of the same type, the value of A_{eff}, as well as its dependency on the operational pressure, may be different.

4.3. Estimation of associated uncertainties

The standard uncertainty introduced by each parameter involved in the computation of the effective area is estimated. These uncertainties are tabulated in tables 5 and 6 for the gauge and absolute modes, respectively, for all five devices and the maximum operating pressure of each device. All values are in parts per million (ppm) and they are computed based on equation (8). The total uncertainty, based on equation (9), is also provided. Next, each introduced uncertainty is separately discussed for different scenarios.

Starting with the dimensional uncertainty it is seen that, as expected, uncertainties introduced from dimensional measurements are, in general, significant. For devices where the uncertainty of the dimensional measurements is of the order

Table 5. Theoretical standard uncertainty (ppm) for all PCAs at maximum operation pressure in the gauge mode.

PCA	FPG8601 (PTB)	FPG8601 (RISE)	FPG8601 (INRiM)	FRS4 (CMI)	FRS5 (PTB)
Dimensional uncertainty	1.07	8.00	1.04	6.26	0.57
Acc. coef. ($\alpha = 0.9$)	0.11	0.47	0.38	0.00	0.00
Acc. coef. ($\alpha = 0.8$)	0.27	1.02	0.81	0.01	0.00
Temperature change (± 1 K)	0.00	0.01	0.01	0.00	0.00
Temperature change (± 2 K)	0.01	0.02	0.02	0.00	0.00
Model equation (BGK versus BE)	0.03	0.11	0.09	0.00	0.00
Relative humidity (50%)	0.00	0.01	0.01	0.00	0.00
Total uncertainty	1.11	8.07	1.32	6.26	0.57

Table 6. Theoretical standard uncertainty (ppm) for all PCAs at maximum operation pressure in the absolute mode.

PCA	FPG8601 (PTB)	FPG8601 (RISE)	FPG8601 (INRiM)	FRS5 (PTB)
Dimensional uncertainty	1.07	8.00	1.04	0.57
Accom. coef. ($\alpha = 0.9$)	0.35	1.20	1.13	0.17
Accom. coef. ($\alpha = 0.8$)	0.75	2.44	2.31	0.30
Temperature change (± 1 K)	0.01	0.05	0.05	0.01
Temperature change (± 2 K)	0.03	0.11	0.10	0.02
Model equation (BGK versus BE)	0.05	0.25	0.19	0.03
Relative humidity (50%)	0.01	0.04	0.04	0.01
Total uncertainty	1.31	8.38	2.55	0.65

of 25–30 nm, the uncertainty introduced in A_{eff} is about 1 ppm or less, depending on the device. When dimensional uncertainty is higher, the contribution is also higher and can reach up to 8 ppm. Along with the uncertainty of the dimensional measurement, the effect of the limited number of the measurement angles was studied and, in tables 5 and 6, is included in the dimensional uncertainty. It is noted that the exact value depends not only on the dimensional uncertainty but also the average piston-cylinder radius.

Concerning the uncertainty introduced by the accommodation coefficient, it is noted that in most cases $\alpha = 1$ (this is the reference value for the estimation of A_{eff}). In some cases, when the surface is treated, α may be slightly reduced. Here, two scenarios have been examined: (a) $\alpha = 0.9$ and (b) $\alpha = 0.8$. In the first scenario, the maximum deviations are 1.2 ppm and 0.47 ppm for the absolute and gauge operation modes, respectively, and the corresponding values in the second scenario are 2.44 ppm and 1.02, respectively. Taking into consideration that $\alpha = 0.8$ corresponds to a highly polished surface, it may be concluded that the effect of the accommodation coefficient is of moderate importance but not negligible.

Next, the uncertainty introduced by gas temperature variations is examined by considering the deduced changes of the gas properties, namely the most probable velocity and viscosity. Deformations of the piston and the cylinder due to material's thermal expansion are not considered, since the temperature fluctuations are small and, because the thermal expansion correction is usually applied to the effective area during piston gauge operation considering the PCA temperature. Two scenarios are examined: (a) $\Delta T = \pm 1$ K and (b) $\Delta T = \pm 2$ K. In all cases, the deviations are less than 0.11 ppm. Since the operation of the devices is under isothermal conditions and the pressure range is small with very weak compressibility effects, temperature variations larger than 2 K are not expected. Therefore, the temperature effect on the uncertainty of A_{eff} is negligible.

The uncertainty due to the implementation of the BGK kinetic model equation instead of the BE is also examined. To achieve that, the flow has been simulated by solving the linearized BE and comparisons with the corresponding BGK results have been performed. In the absolute operation mode, where gas rarefaction effects are stronger, the maximum deviation is about 0.25 ppm, while in the gauge operation mode, where the gas is more dense, the maximum value is 0.11 ppm. It is clear that the BGK model does not introduce any significant error in the calculations of A_{eff} and the BGK equation can be considered as a reliable tool in the case of isothermal flows.

The gas flowing in the gap between the piston and the cylinder in the reference case is considered to be dry N_2. In fact, under real conditions it contains 50% relative humidity. To judge if the assumption of dry N_2 has a significant impact on the results, simulations have been performed for all devices using the equivalent gas theory [27]. Now the gas mixture is considered as a single equivalent gas and its properties are the weighted mean average of the properties of the mixture components. It has been found that in all cases the deviations are smaller than 0.04 ppm. Although strictly speaking the equivalent single gas theory is valid in the slip and viscous regimes and its accuracy is gradually reduced in the transition or the free molecular regimes, it may be safely concluded that the dry gas assumption has a negligible effect on the computation of the effective area.

Finally, based on all these uncertainties the total uncertainty for each PCA at its maximum operation pressure is tabulated in the last lines of tables 5 and 6. It is computed via equation (9) as the Euclidean norm of all uncertainty contributions for the worst-case scenario. For all five assemblies, the total uncertainty is less than 10 ppm. The uncertainty of the dimensional measurements is the most important parameter followed by the accommodation coefficient, while the uncertainties due to variations in the gas temperature, the use of the

BGK model and the humidity content are negligible. It is concluded that, by implementing kinetic modeling tools, accurate values of A_{eff} in the operation pressure range of 1 Pa–15 kPa for both the absolute and gauge operational modes can be obtained. Furthermore, provided that dimensional measurements with small uncertainty are recovered, pressure measurements of high accuracy can be ensured.

5. Concluding remarks

In the present work, the effective area of three FPG8601, one FRS4 and one FRS5 in the whole operational pressure range of each device varying between 1 Pa and 15 kPa has been computed. Geometrical data for the PCAs have been provided by PTB, RISE, INRiM and CMI. Since the flow is under rarefied conditions, modeling has been based on the BGK model equation, while the typical Dadson and CFD approaches have been complimentary applied only in the viscous regime.

It has been found that the effective area is strongly affected by the geometry of the device and the flow conditions, and its estimated value, as well as its dependency on pressure, may be different even for devices of the same type. Furthermore, an uncertainty analysis has been performed. It is concluded that the main source of uncertainty is the dimensional measurements of the piston and the cylinder, followed by the accommodation coefficient characterizing the gas-surface interaction, while the effect of other flow and modeling parameters is negligible. In all cases, the total standard uncertainty of the effective area has been found to be less than 10 ppm indicating that pressure measurements of high accuracy can be ensured. It is noted that, since the effective area is computed based solely on simulations, the FPG and the FRS piston gauges characterized in this way can serve as primary pressure standards.

Finally, it is noted that a comparison between the computed effective areas based on the present analysis with the corresponding experimental ones obtained by the NMIs taking into account the associated uncertainties is in progress. The objective is to determine the expected accuracy when the PCAs are used as primary and secondary pressure standards.

Acknowledgments

The contribution of Research Institutes of Sweden (RISE), Istituto Nazionale di Ricerca Metrologica (INRiM) and Czech Metrology Institute (CMI) having provided the dimensional data for their FPG8601 and FRS4 PCAs is greatly acknowledged. This work has received funding from the EMPIR programme co-financed by the Participating States and from the European Union's Horizon 2020 research and innovation programme with number 14IND06 pres2vac and title 'Industrial standards in the intermediate pressure-to-vacuum range'.

ORCID iDs

Ahmed S Hashad https://orcid.org/0000-0001-6426-8696

References

[1] Ooiwa A 1994 Novel nonrotational piston gauge with weight balance mechanism for the measurement of small differential pressures *Metrologia* **30** 607–10
[2] Delajoud P and Girard M 2002 A force balanced piston gauge for very low pressure *Proc. NCSL Int. Workshop & Symp. (San Diego)*
[3] Krajícek Z, Bergoglio M, Jousten K, Otal P, Sabuga W, Saxholm S, Pražák D and Vicar M 2014 Final report on EURAMET.M.P-K4.2010: key and supplementary comparison of national pressure standards in the range 1 Pa–15 kPa of absolute and gauge pressure *Metrologia* **51** 07002
[4] Ricker J, Hendricks J, Bock T, Pražák D, Kobata T, Torres J and Sadkovskaya I 2017 Final report on the key comparison CCM.P-K4.2012 in absolute pressure from 1 Pa to 10 kPa *Metrologia* **54** 07002
[5] Bock T, Ahrendt H and Jousten K 2009 Reduction of the uncertainty of the PTB vacuum pressure scale by a new large area non-rotating piston gauge *Metrologia* **46** 389–96
[6] FPG8601™/VLPC™ 2007 Operation and maintenance manual, DH Instruments a Fluke Company https://us.flukecal.com/elqNow2/elqRedir.htm?ref=http://www.dhinstruments.com/supp1/manuals/fpg/550122.pdf
[7] Rendle C G and Rosenberg H 1999 New absolute pressure standard in the range 1 Pa–7 kPa *Metrologia* **36** 613–5
[8] Perkin M *et al* 1999 Comparison of European differential pressure standards in the range 3 Pa–1000 Pa *Metrologia* **36** 1–7
[9] Tesar J, Pražák D, Stanek F, Repa P and Peksa L 2007 Ensuring primary realization of pressure unit in the vacuum range without typically utilized static expansion system *Vacuum* **81** 785–7
[10] Stanek F and Krajícek Z 2003 Státní etalon přetlaku, podtlaku a diferenčního tlaku v plynném médiu *Metrologie* **12** 15–21
[11] Stanek F, Krajícek Z, Tesar J and Pražák D 2008 Státní etalon vakua *Metrologie* **17** 17–24
[12] Hashad A S, Ehlers S, Jusko O and Sabuga W 2019 Characterization of a force-balanced piston gauge as a primary pressure standard *Measurement* **131** 723–9
[13] Dadson R S, Lewis S and Peggs G N 1982 *The Pressure Balance: Theory and Practice* (London: HSMO)
[14] Cercignani C 1975 *Theory and Application of the Boltzmann* (Edinburgh: Scottish Academic Press)
[15] Sharipov F and Seleznev V 1998 Data in internal rarefied gas flows *J. Phys. Chem. Ref. Data* **27** 657–706
[16] Jousten K 2008 *Handbook of Vacuum Technology* (Weinheim: Wiley)
[17] Naris S, Tantos C and Valougeorgis D 2014 Kinetic modelling of a tapered Holweck pump *Vacuum* **109** 341–8
[18] Kandlikar S, Garimella S, Li D, Colin S and King M R 2013 *Heat Transfer and Fluid Flow in Minichannels and Microchannels* (Amsterdam: Elsevier)
[19] Sharipov F 2016 *Rarefied Gas Dynamics. Fundamentals for Research and Practice* (New York: Wiley)
[20] Sharipov F, Yang Y, Ricker J E and Hendricks J H 2016 Primary pressure standard based on piston-cylinder assemblies. Calculation of effective cross sectional area based on rarefied gas dynamics *Metrologia* **53** 1177–84
[21] Sabuga W, Sharipov F and Priruenrom T 2011 Determination of the effective area of piston-cylinder assemblies using rarefied gas flow model *PTB-Mitt.* **121** 260–2
[22] Ooiwa A and Ueki M 1993 Development of novel air piston gauge for medium and fine differential pressure measurement *Vacuum* **44** 603–5
[23] Rendle C G and Rosenberg H 1993/1994 A large area piston gauge for differential and gauge pressure from zero to 3.2 kPa *Metrologia* **30** 611–3

[24] Breyiannis G, Varoutis S and Valougeorgis D 2008 Rarefied gas flow in concentric annular tube: estimation of the poiseuille number and the exact hydraulic diameter *Eur. J. Mech.* B **27** 609–22
[25] Sabuga W 2011 Pressure measurements in gas media up to 7.5 MPa for the Boltzmann constant redetermination *PTB-Mitt.* **121** 247–55
[26] Pantazis S, Valougeorgis D and Sharipov F 2014 End corrections for rarefied gas flows through circular tubes of finite length *Vacuum* **101** 306–12
[27] Valougeorgis D, Vargas M and Naris S 2016 Analysis of gas separation, conductance and equivalent single gas approach for binary gas mixture flow expansion through tubes of various lengths into vacuum *Vacuum* **128** 1–8